Solution structure and counterion condensation of carboxymethyl cellulose in organic solvents.

Anish Gulati,[1] Lingzi Meng,[2] Can Hou,[1] Takaichi Watanabe,[3] and Carlos G. Lopez[2]
[1)]*Institute of Physical Chemistry, RWTH Aachen University, Landoltweg 2, 52056 Aachen, Germany, European Union*
[2)]*Materials Science and Engineering Department, The Pennsylvania State University, State College, 16802, US*
[3)]*Department of Applied Chemistry, Graduate School of Environmental, Life, Natural Science and Technology, Okayama University, 3-1-1, Tsushima-naka, Kita-ku, Okayama 700-8530, Japan*

(*Electronic mail: cvg5719@psu.edu)

We report scattering (SANS and SAXS) and electrical conductivity data for aqueous and organic solutions of carboxymethyl cellulose with tetrabutylammonium counterions. For SANS in deuterated solvents the contrast is heavily dominated by the hydrogen-rich counterions while for SAXS, the polymer backbone has a more significant contribution to the scattering signal. The correlation length calculated from the SAXS measurements follows a scaling law of $\xi \propto c^{-1/2}$ while that measured by SANS displays a weaker exponent at higher concentrations for solvents of high dielectric constants. These results indicate a decoupling in the characteristic lengthscales of fluctuations of the polymer backbone and counterions at high polyelectrolyte concentrations. The stretching parameter calculated from the correlation length indicates highly stretched local conformation for TBACMC in water and several high dielectric constant solvents, consistent with the semiflexible nature of the cellulose backbone. In solvents of lower dielectric permittivity, the chains display a higher degree of local coiling. Combining electrical conductivity and scattering data we find that the fraction of monomers bearing a dissociated charge is nearly independent of concentration and approximately proportional to the reciprocal of the Bjerrum length of the solvent, as expected by the Oosawa-Manning model.

I. INTRODUCTION

Polyelectrolytes are a class of ion-containing polymers for which all the ionic groups bear charges of the same sign.[1–4] The presence of charged groups on the polymer backbone enhances their solubility in polar solvents and allows them to form complexes with oppositely charged species.[5–8] By independently tuning the polymer backbone and counterions, orthogonal functionality can be introduced, allowing specific properties such as responsiveness to environmental factors (e.g. temperature, pH and ionic strength).[9,10]

Water is without a doubt the most important solvent for charged polymers due to its relevance to living organisms, where polyelectrolytes play a role in many physiological processes.[11–15] Because of this, the vast majority of the experimental polyelectrolyte literature focuses on the properties of aqueous solutions.[16,17] The lack of comprehensive studies on polyelectrolytes in non-aqueous media results in two limitations in our fundamental understanding of polyelectrolyte solutions. First, the role of solvent permittivity on the properties of polyelectrolytes[18–20] has not been systematically studied, with most work being carried out at a fixed dielectric constant of $\varepsilon \simeq 78$. Second, the influence of polymer and counterion-solvent interactions[21–24] on the thermodynamics, structure and rheology of polyelectrolytes remains largely unexplored.[17] Understanding how dielectric constant and other solvent properties affect charged polymers is relevant for applications such as batteries[25] and membranes.[26–30]

The dielectric constant of the solvent sets the strength of electrostatic interactions between charges in solution. In the absence of electrostatic screening, the Coulomb energy (U_C) for a pair of oppositely charged ions is $U_C/k_BT = -l_B/r$, where k_B is Bolztmann's constant, T the absolute temperature and l_B the Bjerrum length. The Bjerrum length is the distance at which the electrostatic and thermal energies of a pair of monovalent ions in solution are equal:

$$l_B = \frac{e^2}{4\pi k_B T \varepsilon_0 \varepsilon}$$

where e is the electrostatic unit of charge, ε is the dielectric constant or relative permittivity of the solvent and ε_0 is the vacuum permittivity.

The coupling parameter (u) is defined as the ratio between the Bjerrum length to the distance between ionic groups on the backbone. The distance between charges is given by the ratio of the length of a chemical monomer (b) and the number of charges per monomer unit (n):

$$u = nl_B/b$$

The theory of counterion condensation[31–33] predicts that when the coupling parameter exceeds unity, counterions condense onto the polymer backbone, neutralising the ionic groups, so as to bring the effective charge density to a value of one charge per Bjerrum length. The effective charge density of the backbone (μ_{eff}) is:

$$\mu_{eff} = \begin{cases} e \cdot n/b & \text{if } u < 1 \\ e/l_B & \text{if } u > 1 \end{cases} \quad (1)$$

Counterion condensation is essential to understanding polyelectrolyte solutions because virtually all polyelectrolyte properties, from osmotic pressure or charge transport to the rheological properties of solutions are dependent on the effective charge of the chains.[17,34,35]

While Oosawa and Manning derived their theories for single chains (i.e. solutions in the infinite dilution limit), results by Wandrey et al[36,37] show that the Oosawa-Manning threshold for salt-free solutions applies only in the semidilute regime. Below the overlap point, the fraction of free counterions increases upon dilution, in agreement with the two-phase model of Liao et al.[38]

Nyquist el al[39] find broad agreement with Manning's theory but predict a less sharp dependence of the fraction of condensed counterions on the bare charge density. Theoretical work by Muthukumar and co-workers[40–42] expects strong deviations from the Oosawa-Manning model for flexible chains. In brief, their theory predicts that because counterion adsorption influences chain conformation, a self-consistent calculation of the free energy of the polyelectrolyte (chain and counterions) is necessary to estimate the fraction of free counterions.[43] These works also predict that the dielectric mismatch, which is proportional to the relative difference between the dielectric constant in the bulk and around the polymer chains, can significantly alter counterion adsorption profiles. When plotting f as a function of Bjerrum length at constant dielectric mismatch, Muthukumar and co-workers observe much sharper dependences than the Manning model. A difficult that arises in checking these predictions is the lack of experimental methods to quantify the dielectric mismatch.

Equation 1 can be experimentally tested in two ways: first, altering the chemical composition of the backbone, the value of n can be changed. Dou and Colby quaternized poly(2-vinyl pyridine) to different degrees and used electrical conductivity measurements to evaluate the effective charge density of the chain in semidilute ethylene glycol solutions.[44] Their results agree with several aspects of the OM model: The $\mu_{eff} \propto n$ and $\mu_{eff} \propto n^0$ at low and high charge density are approximately observed, but the cross-over between these two regimes was however broader than expected by Eq. 1. The effective charge density in the high charge density region is close to e/l_B as expected by Eq. 1. Kowblansky and Zema[45] studied the activity of counterions of copolymers of acrylic acid and acrylamide with varying charge density, finding reasonable agreement with Manning's theory.

The second approach to test Eq. 1 is to keep the chemical composition of the polymer constant (i.e. constant n) and vary the dielectric constant of the solvent. Here, fewer studies, mostly relying on indirect measurements of the effective charge fraction have been performed: in one study, Beer et al fit a Flory-theory to radius of gyration vs. added salt concentration data for polyvinyl pyridine derivatives, which allowed them to extract the effective charge fraction and intrinsic excluded volume.[18] This yielded an unusual dependence of $\mu_{eff} \simeq (\varepsilon - 16)^{1/2}$, which does not agree with Oosawa-Manning. In another study, Lopez et al[17] used the scaling theory[46] to calculate f from overlap concentration data of two poly(ionic liquids).[19,47] A stronger than anticipated dependence of $\mu_{eff} \propto \varepsilon^{1.6}$ was found. This relationship was obtained on the assumption that all solvents considered act as θ solvents for the backbone, which could not be verified.

Studying non-aqueous solvents can yield insight into the nature of electrostatic forces in polyelectrolyte solutions. This is challenging because of the limited solubility of most polyelectrolytes in non-aqueous media.[48,49] One way of overcoming this difficulty is to increase the affinity of the counterions for the solvent.[50] This approach was pioneered by Ono and co-workers[51–54] and Chen et al[55] to develop cross-linked polyelectrolyte networks with high absorption capacity for apolar solvents. More recently, the tetra-alkyl-ammonium salts of polystyrene sulfonate and carboxymethyl cellulose we found to be soluble in many protic, polar solvents.[20,56,57]

In this paper, we study the structural and transport properties of tetrabutyl ammonium carboxymethyl cellulose (TBACMC) in different solvents. SANS and SAXS measurements are used to gain insight into the structure of the polymer mesh and the distribution of counterions and conductivity data allow us to establish the fraction of free counterions as a function of the dielectric constant of the solvent.

A. Previous work on CMC solutions

Carboxymethyl cellulose is a semiflexible, weak, anionic ether of cellulose made by reacting chloroacetic acid with activated cellulose.[58–60] The average number of carboxymethyl groups (out of three hydroxyl groups in the glucose unit) per monomer is known as the degree of substitution or DS. Commercially, carboxymethyl cellulose is used as the sodium salt (NaCMC) with DS $\gtrsim 0.7$ as required for solubility in water. Higher substitution degrees are used to ensure a more regular substitution pattern which prevent gelation of CMC at high polymer concentrations.[61–63] The many applications of CMC in the food, pharmaceutical, paper and oil industries as well as potential applications in new technologies[64–66] have lead to extensive investigations into its physical properties.

1. Counterion condensation

The first systematic studies on the effective charge fraction of NaCMC used potentiometry and osmotic pressure to determine the activity and osmotic coefficients of CMC solutions with various monovalent and divalent counterions.[67–73] The effective charge of the chain was found to be inversely proportional to the counterion valence, as predicted by the Oosawa-Manning model. For a given counterion valence, the counterion type has a large influence on the degree of ion pair formation[74–79] but not on the fraction of free counterions.[67,71,80] The effective charge fractions obtained from these studies were reviewed recently and found to qualitatively agree with Oosawa-Manning.[80]

Cametti and co-workers[81,82] studied the dielectric response of two NaCMC polymers in aqueous solutions. The DC conductivity was used to estimate the fraction of free counterions as a function of polymer concentration. For sufficiently dilute solutions, all counterions were found to be dissociated. Solutions above the overlap concentration showed an approximately concentration-independent fraction of free counterions, and the effective charge was similar to the Oosawa-Manning threshold. Beyond a critical concentration,

counterion condensation increased with increasing concentration, which was assigned to a cross-over to the concentrated regime. Scattering data for CMC[83] and PSS[84] with organic counterions suggest counterion delocalisation at high polymer concentrations, which appears inconsistent with increased condensation. The complex permittivity of NaCMC solutions at intermediate frequencies followed scaling laws with concentration similar to those of flexible polyelectrolytes.[85] The fraction of free counterions estimated by applying the scaling model to dielectric increment data gave a similar result to that obtained from electrical conductivity, see ref. [80].

The electrical conductivity of sodium carboxymethyl cellulose in DI water solutions and mixtures of water and organic solvents has been investigated extensively by Das and co-workers[86–93], who applied the model of Colby et al[85,94] to calculate the fraction of free counterions as a function of degree of substitution, polymer concentration and non-solvent fraction. One limitation of these works is that in order to calculate the correlation length, which is needed to fit the model of Colby et al to conductivity data, the authors relied on the scaling theory for flexible polyelectrolyte solutions. In their calculation they assume chain flexibility on lengthscales larger than the chemical monomer size ($\simeq 0.5$ nm), which is unrealistic for a semiflexible polymer like CMC. In a recent study, we measured the correlation length using small angle x-ray scattering (SAXS)[49] in water and water/non-solvent mixtures which allowed us to more directly calculate the fraction of free counterions. The results showed that the fraction of charged monomers was nearly independent of polymer concentration and inversely proportional to the Bjerrum length, as anticipated by the Oosawa-Manning theory, but the charge density was found to be $\simeq \times 1.5$ lower than the OM threshold.

2. *Solution structure and rheological properties*

Several studies employing scattering methods[49,62,83,95,96] have shown that the local conformation of NaCMC in water is rod-like, as expected due to the semiflexible nature of the cellulose backbone. The scattering patterns of alkaline salts in aqueous solutions display a correlation peak, characteristic of salt-free polyelectrolyte solutions, over the entire concentration range studied. The correlation length (ξ) was found to be proportional to $c^{-1/2}$, in agreement with the prediction of the scaling theory.[46,97] For tetra-alkyl-ammonium salts of CMC, the SANS spectra displays a peak at low concentrations which morphs into a broad shoulder feature as the concentration is increased. The SAXS signal on the other hand showed clear peaks over the entire concentration range following the $\xi \propto c^{-1/2}$ dependence. Because the SANS signal is dominated by the counterion contribution, this likely results from a decoupling of the polymer backbone and counterion concentration fluctuations, a feature that has been observed, albeit to a smaller extent, for TMAPSS in water.[84]

The structure of NaCMC and CsCMC in mixtures of water and ethanol, 2-propanol and acetone was studied by small angle x-ray scattering.[49] The addition of a non-solvent decreased the effective charge of the backbone but the correlation length was independent of solvent composition except when solutions were close to the solubility boundary. The independence of the scattering peak on the effective charge fraction of the chain is expected by the scaling model when the bare Kuhn segment of the chain ($\simeq$ 10 nm for NaCMC) is much larger than the Bjerrum length of the solvent ($\simeq$ 1-2 nm for the solvent mixtures studied).[49]

Other studies on the behaviour of NaCMC in mixed solvents have focused on understanding the rheological properties of solutions[98–102]. Rozanski and co-workers showed that for sufficiently high polymer concentrations and/or low degrees of substitution, addition of a non-solvent can lead to a sol-gel transition.[100,101] The non-solvent induced gelation likely arises from a combination of two phenomena: first, as non-solvent is added and the effective charge of the backbone decreases, the energetic barrier for two segments to approach each other decreases, thereby facilitating inter-chain associations. Second, the as the solvent quality worsens, unsubstituted regions of the cellulose backbone experience stronger attractions.[101]

In this manuscript, we study the scattering properties of TBACMC in several organic solvents and water. The scattering data are used in combination with electrical conductivity measurements to estimate the fraction of free counterions over a relatively broad range of dielectric permittivities. Our results show reasonable agreement with the Oosawa-Manning condensation threshold and yield new insights into the spatial correlations between monomers and counterions.

II. SCATTERING OF POLYELECTROLYTE SOLUTIONS

The SANS or SAXS intensity of a polyelectrolyte solution can be expressed in terms of the structure factors of the monomers and counterions as:[105]

$$I(q) = \rho_m \overline{b}_m^2 S_{mm}(q) + 2\sqrt{\rho_m \rho_c}(\overline{b}_m \overline{b}_c) S_{mc}(q) + \rho_c \overline{b}_c^2 S_{cc}(q) \tag{2}$$

where $S(q)_{m,m}$, $S(q)_{m,c}$ and $S(q)_{c,c}$ are the partial structure factors, for monomer-monomer, monomer-counterion and counterion-counterion correlations respectively. The concentrations in units of number per unit volume are: ρ_m and ρ_c, where the m subscript refers to the monomer and the c subscript refers to the counterion. See refs. [105,106] for details.

The contrast factors in equation 2 are:

$$\overline{b_i} = b_i - b_s \frac{v_i}{v_s} \tag{3}$$

where b_i and v_i are the coherent scattering length and volume of the unit respectively. The coherent scattering length is the sum of the coherent scattering length of each isotope in the scattering unit. For SANS, values of b_i were taken from the NIST website.[107] For SAXS, b_i is the product of the number of electrons of the scattering unit and the electron scattering length. The subscript s refers to the solvent and $i = c$ or $i = m$ refers to the counterion or monomer.

In an earlier study[83] we estimated the molar volumes of the TBA^+ and CMC^- from density measurements. However,

Solvent	η_s [mPas]	σ [μS/cm]	ρ [g/cm^3]	c_{res} [M]	ε [-]
N-methyl formamide (NMF)	1.681	54	0.9988	5×10^{-4}	182
N-methyl acetamide (NMA)	3.65	10.5	0.9371	7×10^{-5}	172
Water	0.89	2	0.9970 (0.9970)	4×10^{-6}	78
Dimethyl sulfoxide (DMSO)	1.987	0.5437	1.101 (1.0956)	2×10^{-6}	47.2
Dimethyl formamide (DMF)	0.794	1.1825	0.9445 (0.9444)	2×10^{-6}	38.3
Ethylene Glycol (EG)	16.1	0.0836	1.1135 (1.1097)	3×10^{-6}	41.4
Methanol (MeOH)	0.544	0.8225	0.7914 (0.7867)	1×10^{-6}	33
Ethanol (EtOH)	1.074	0.1475	0.7893 (0.7856)	4×10^{-7}	25.3
1-propanol (PrOH)	1.945	0.100	0.7997 (0.7996)	4×10^{-7}	21
1-butanol (BuOH)	2.544	0.1795	0.8095	10^{-6}	17.8

TABLE I. Properties of solvents used in this study. [a] properties at T = 35 °C. Dielectric constant and limiting molar conductivity data are values taken from the references indicated. Conductivity is measured by us. Densities are values from [103] and measurements for our solvents are in brackets. The residual salt concentration is calculated using Eq. 4. Density and viscosity data for NMF are from ref. [104]

these calculations did not take into account electrostriction of the solvent. Here we use a molar volume of 274 mL/mol for the TBA^+ ion, following ref. [108] and 134 mL/mol for the CMC^- ion. SANS experiments were conducted using deuterated solvents and for all systems studied the prefactor to the counterion structure factor ($\rho_c\bar{b}_c^2$) dominates over the backbone's ($\bar{b}_m^2$). For the solvents studied with SAXS the opposite is true and the prefactor to $S(q)_{m,m}$ is 2-3 orders of magnitude larger than for $S(q)_{c,c}$.

III. MATERIALS AND METHODS

Materials: NaCMC was purchased from Sigma-Aldrich, with a nominal molar mass of 250 kg/mol and degree of substitution DS $\simeq$ 1.2. The molar mass was determined from the intrinsic viscosity in 0.1 M NaCl in an earlier study to be $\simeq$ 240 kg/mol. The degree of substitution was measured by back titration of the acid form as DS = 1.3. Spectra/Por dialysis membranes with a MWCO of 6-8 kDa were used and were purchased from VWR. Solvents were purchased from VWR or Sigma-Aldrich except for NMF which was from FUJIFILM Wako Pure Chemical Corporation.

Preparation of CMC salts: NaCMC was dialysed against DI water and freeze dried. The freeze dried polymer was used to prepare the NaCMC solutions. The TBACMC used in this study is the same as in our previous work, see ref [83]. In brief, the NaCMC was converted to its acid form (HCMC) by adding excess HCl followed by dialysis against DI water. The HCMC was freeze dried, neutralised with excess TBAOH, dialysed against DI water and freeze dried.

Sample preparation: The dialysed and freeze dried CMC salts were stored in the vacuum freeze dryer for $\sim$ 24 hours before any samples were prepared. The samples were prepared in polypropylene microcentrifuge tubes, previously washed with DI water and dried at 60 °C. All the sample components were added by weight using a weighing balance with a least count of 0.1 mg and, therefore, a typical error of $\pm$0.05 mg. Solvents were used as received, without further purification.

Densitometry: The density measurements were performed using the Anton Paar DMA 5000 densitometer with a least count of 10^{-6} g cm^{-3}. The accuracy of the instrument was checked using DI water.

Conductivity and pH: Conductivity measurements were made using the Mettler Toledo S47 SevenMulti conductivity meter. The temperature was maintained at 25$\pm$0.1 °C using a continuously stirred water bath and heating plate system provided with temperature probes at different points to ensure the temperature accuracy. On achieving the required temperature, the mean value of four measurements was taken. pH measurements were made using the Metrohm 744 pH meter.

Small-Angle Neutron Scattering: The SANS measurements were carried out at the D11 beamline at Institut Laue Langevin, Grenoble, France. Measurements were performed at five different sample-to-detector distances (1.7 m, 5.5 m, 8 m, 12 m and 28 m), depending on the sample, covering a q-range of 0.002 - 0.55 Å^{-1}. The neutron wavelength was λ = 6 Å for all experiments. Samples were measured in cylindrical (banjo) cells with path lengths of 1 mm, 2 mm or 5 mm depending on polymer concentration. The reduced scattering intensities are tabulated in the supporting information.

Small-Angle X-Ray Scattering: The SAXS measurements were carried out using an in-house instrument and at the SPring-8 synchrotron. The in-house instrument consists of a 3-pinhole S-Max3000 system with a MicroMax002+ X-ray microfocus generator from Rigaku and a 2D multiwire detector with an active diameter of 200 mm. The sample-to-detector distance of 2.6 m was used which covered a q-range of 0.005 - 0.4 Å^{-1} (λ = 1.54 Å, Cu radiation). The samples were measured in sealed 1.5 mm borosilicate capillaries from WJM Glas Müller GmbH. Measurements at the BL40 beamline of the SPring-8 synchrotron facility (Hyogo, Japan) followed the same procedure as in our previous study, see ref. [83] for details. 2 mm capillaries were used and acquisition times were generally between 20 seconds and two minutes, depending on solvent and polymer concentration. The sample-to-detector distance was set to 1 m or 2 m. The reduced scattering intensities, in arbitrary units, are tabulated in the supporting information for all measurements.

All the data were acquired at 25 °C except for measurements in NMA, which were performed at 35 °C to be above its melting point. Measurements of the dialysis bath conduc-

tivity were performed at room temperature ($\simeq 22$ °C).

IV. RESULTS AND DATA FITTING

A. Solvent properties and conductivity measurements

Viscosity, conductivity and density values for the various solvents used in this study are listed in Table I. The densities measured in our laboratory agree with literature values within a few percent, as expected for the solvent grades used. All the solvents have relatively low conductivities, with the exception of NMF, which is known to have a relatively high content of ionic impurities.[109–111] For deionised water, a conductivity of $\simeq 2$ μS/cm is usually taken to correspond to a residual salt concentration of $\simeq 4\times10^{-6}$ M, estimated from the pH of the solution.[112] Lacking information on the type of ionic impurities in our samples, we assume they are common monovalent salts such as alkaline halides. Such monovalent ions usually have limiting ionic conductances of $\lambda \simeq 6\pm1$ mS m^2/mol and the conductivity of a 1 mM solution is $\simeq 150$ μS/cm.[113] An approximate value for the residual salt concentration (c_{res}) can be obtained by assuming the conductivity to be proportional to the c_{res} and inversely proportional to the solvent's viscosity:

$$c_{res}\ [\mathrm{mM}] \simeq \frac{\eta_{solvent}}{\eta_{water}}\frac{\sigma_{solvent}}{150} \qquad (4)$$

where $\eta_{solvent}$ and σ are the viscosity and conductivity in μS/cm of the solvent respectively.

The residual salts for the various solvents studied, calculated using eq. 4 are listed in table I. For most solvents, the residual salt concentration is in the range of a few micromolars. N-methyl-formamide and N-methyl-acetamide have by higher c_{res}, approaching the milimolar range. For a discussion of impurities in NMF, see ref. [110]

The specific conductance ($\Lambda = \sigma/c$) showed a weak concentration-dependence in all solvents, in agreement with earlier reports for alkaline salts of CMC in water or water/non-solvent mixtures.[89–91,93,114] Conductivity data are tabulated in the supporting information.

B. Small-Angle X-ray Scattering

The small angle x-ray scattering patterns of TBACMC in high dielectric constant solvents NMF, NMA and water are plotted in figure 1. In NMF solutions, a correlation peak is observed for all concentrations. This feature is characteristic of polyelectrolytes in low ionic strength solvents and confirms the relatively low content of ionic impurities of the NMF used in this study. For N-methyl-acetamide, the correlation peak is not observed for the lowest concentration measured. This can be assigned either to the presence of residual salts or to the contribution from the low$-q$ upturn which masks the peak. The former scenario would imply a residual salt concentration of $c_S \simeq 0.01$ M (see fig 3 and related discussion) and is incompatible with the relatively low conductivity of the NMA used, see table I.[115]

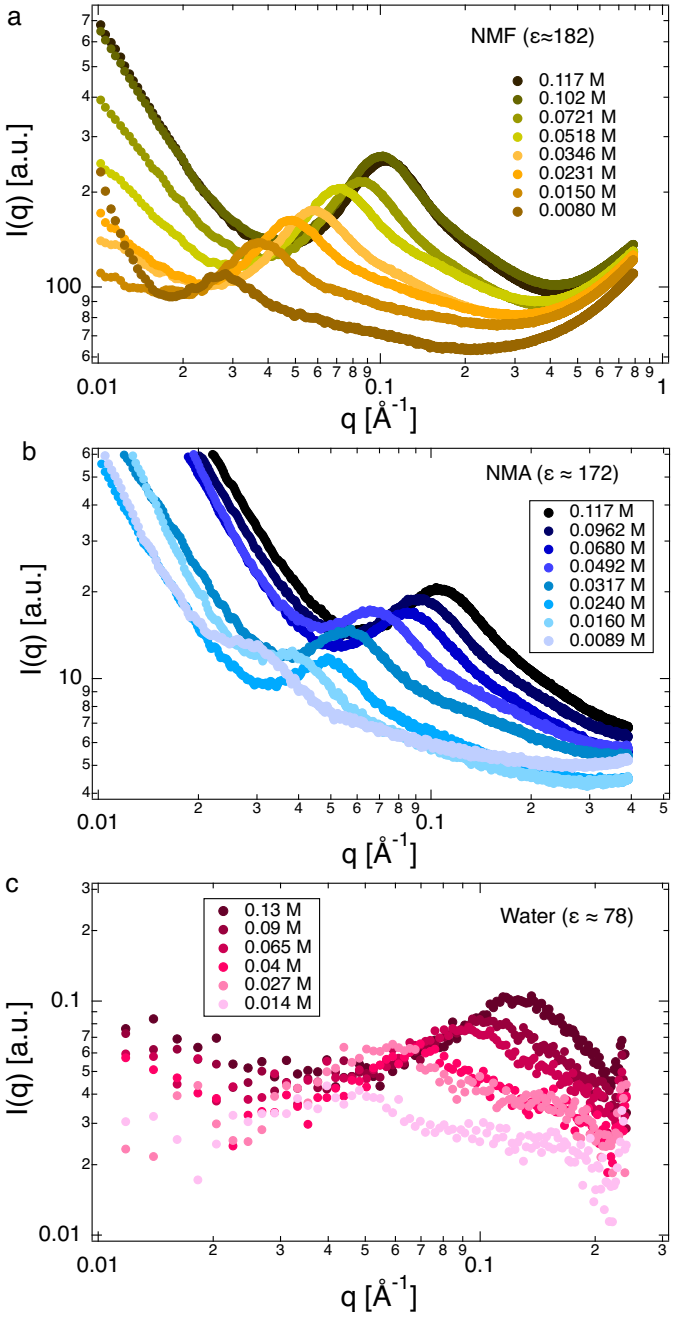

FIG. 1. SAXS profiles for TBACMC solutions in high dielectric constant solvents: N-methyl formamide ($\varepsilon = 182$, $l_B = 0.3$ nm at $T = 25$ °C) (a), N-methyl acetamide ($\varepsilon = 178$, $l_B = 0.31$ nm at $T = 35$ °C) (b), and water ($\varepsilon = 78$, $l_B = 0.71$ nm at $T = 25$ °C) (c). Data for aqueous solutions are from ref. [83], binned (3 to 1) for clarity.

Figure 2 shows SAXS data for TBACMC solutions in three linear alcohols: methanol ($\varepsilon \simeq 32$), ethanol ($\varepsilon \simeq 24$) and 1-propanol ($\varepsilon \simeq 22$). The methanol and ethanol data are measured with the Rigaku in-house instrument. The acquisition times are a few hours, depending on the concentration. Despite the relatively large scatter, the high point density around the maxima means that the peak position can be extracted accurately. The 1-propanol solution data measured at the Spring-8 synchrotron (45 to 120 seconds) display consider-

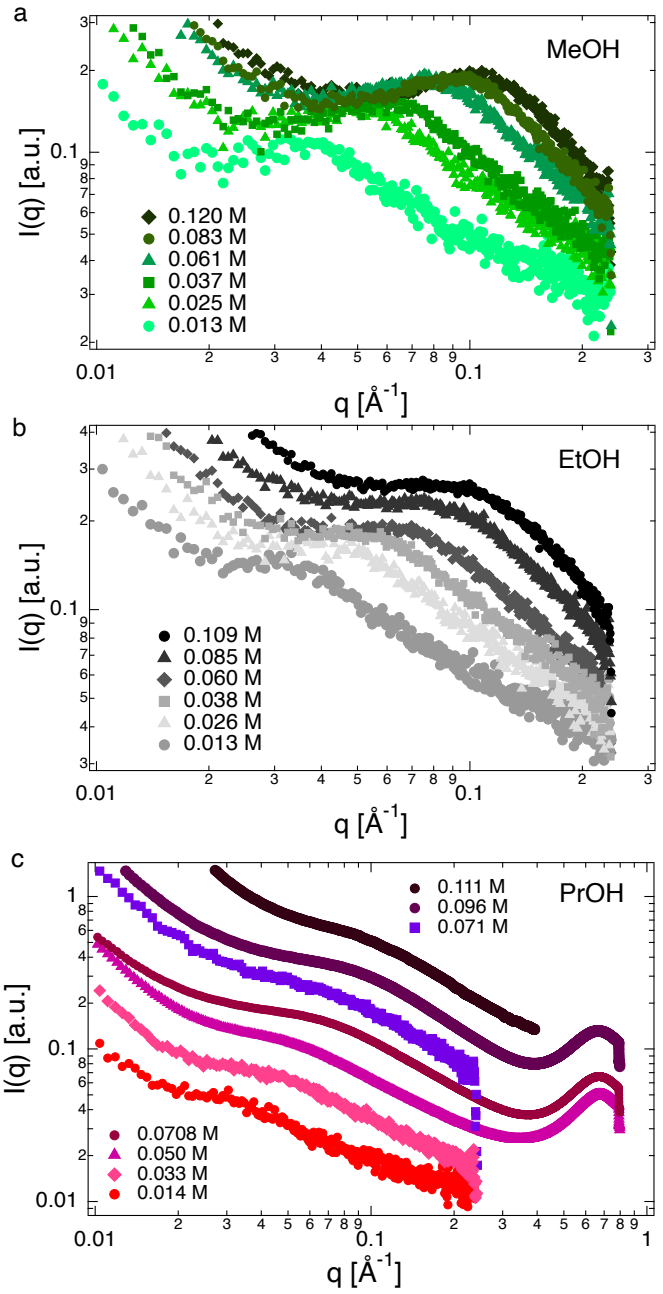

FIG. 2. SAXS profiles for TBACMC solutions in methanol, ethanol and 1-propanol. The top and middle panels are measured on an in-house instrument and the bottom panel is measured at Spring-8. Concentrations are indicated on the legends. Methanol and Ethanol data are measured on the in-house Rigaku instrument. Propanol are measured on the Rigaku instrument ($c = 0.014$, 0.033, 0.071M) or at the SPring-8 synchrotron ($c = 0.111$ M measured with 2 m configuration, others with 1 m configuration). All data are in arbitrary units.

ably less scatter than the samples measured in-house due to the much higher flux of the x-ray beam. The scattering patterns for solutions in methanol display a clear peak over the entire concentration range. For ethanol solutions, the peak at low concentrations morphs into a shoulder at high concentrations and for 1-propanol solutions, no polyelectrolyte peak is observed at any concentration (the peak at $\simeq 0.6$Å^{-1} arises from the solvent contribution and not from the polyelectrolyte chains). Instead, all samples display a broad shoulder and an upturn at low wave-vectors.

1. *Effect of added salt on polyelectrolyte peak*

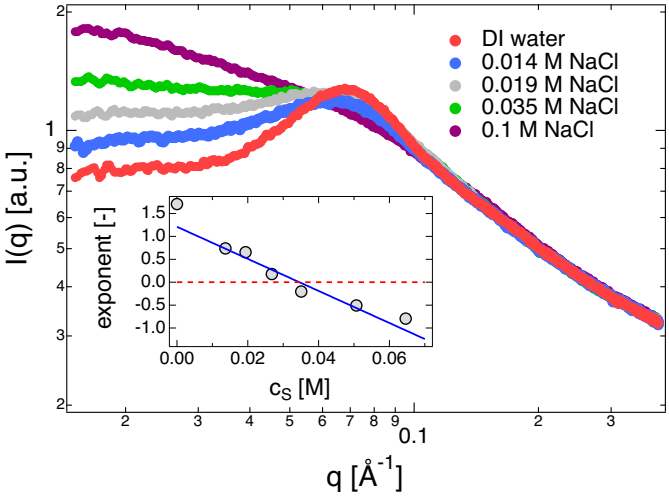

FIG. 3. SAXS curves for NaCMC at $c = 0.054$ M with different added NaCl concentrations, indicated on the legend. The exponents for $q \lesssim q^*$ is plotted as a function of added NaCl in the inset. For $c_S \simeq 0.035$ M, the exponent is approximately zero, which we identify as the transition between peak and shoulder regimes.

The scattering properties of NaCMC solutions in aqueous NaCl solutions were studied as a function of added NaCl concentration. The results are shown in figure 3. As the NaCl concentration increases, the peak first becomes broader and then disappears. We fit power laws to the $q \lesssim q^*$ and $q \gtrsim q^*$ regions, where q^* is the position of the maxima in salt-free solutions. The exponent in the high-q region is independent of c_S and the exponent in the low q region (m_l) increases with increasing c_S, as shown in the inset. The point at which $m_l = 0$ can be identified transition point between peak and shoulder behaviour. This cross-over occurs when $2c_S/(fc) \simeq 2.5$, in qualitative agreement with the scaling model.[46] Results for polystyrene sulfonate[116–118] show a similar value of $fc/(2c_S) \simeq 3$.[80,85,119]

C. Small-Angle Neutron Scattering

Figure 4 plots the SANS scattering intensity of TBACMC in different solvents for a range of concentrations. There are three types of relationships observed between concentration and peak sharpness. In DMSO, the peaks are distinct for all the concentrations studied. The more common behaviour, observed for water, ethanol and methanol, is that the peak disappears at higher concentrations. For DMF, the peak is prominent at high concentrations but vanishes at lower concentrations. We did not measure the conductivity of the deuterated DMF and cannot therefore clearly resolve if the disappearance of the peak at low polymer concentrations is the the result

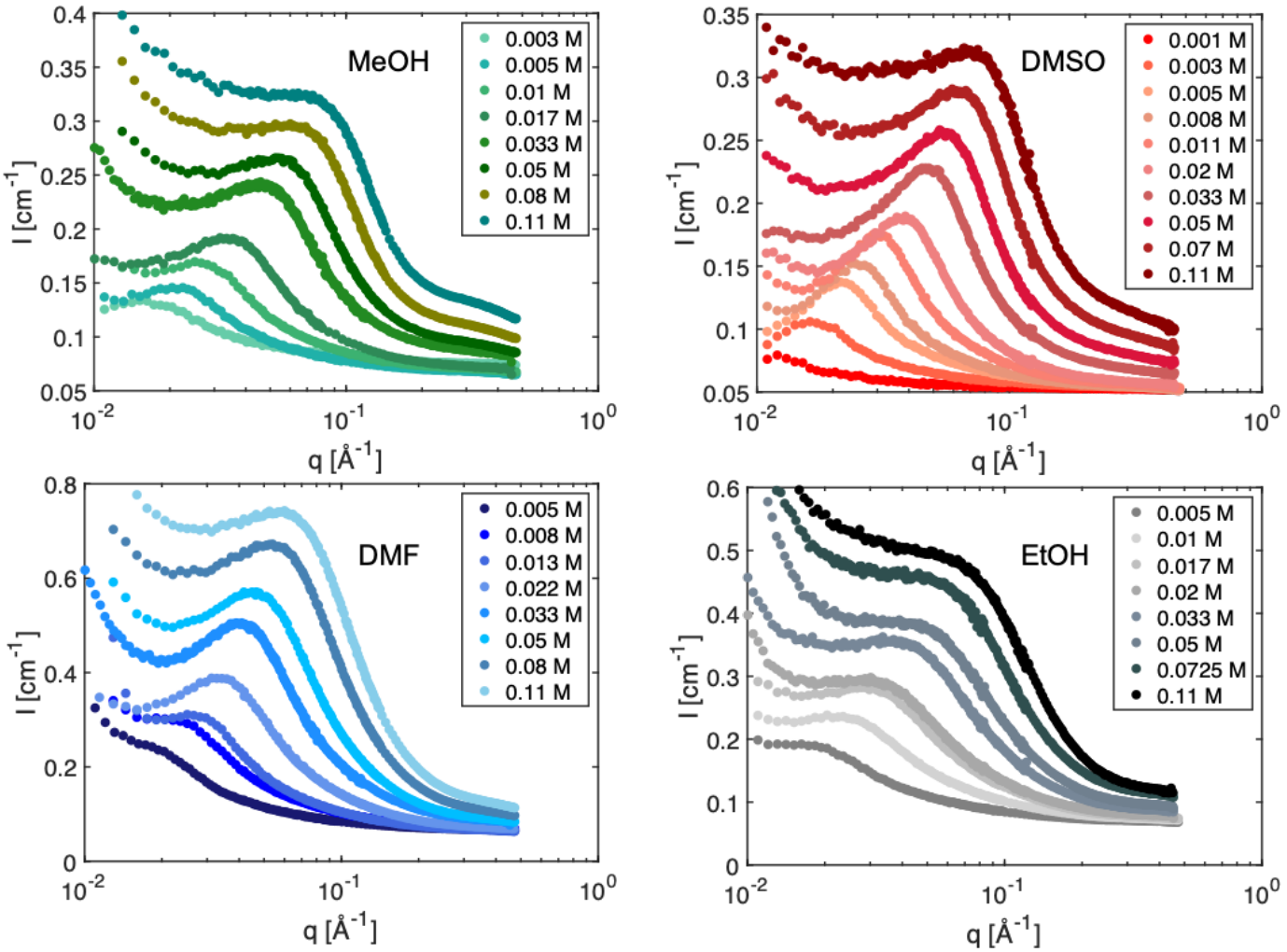

FIG. 4. SANS intensity I as a function of scattering wavevector q for TBACMC in methanol (MeOH), dimethyl sulfoxide (DMSO), dimethyl formamide (DMF) and Ethanol (EtOH) at different concentrations, indicated on the legends. All solvents are deuterated.

of a cross-over to the high salt regime. Common grades of hydrogenated DMF with comparable purity to the deuterated DMF used (99.5%) display low conductivities, corresponding to residual salt concentrations of a few micromolar, which are not sufficient to explain the peak disappearance at around $c \simeq 0.008$ M, see table I. The same holds for ethanol solutions.

We extract the peak positions by fitting a polynomial around the local maxima in the scattering intensity. When no clear maximum is observed, we fit two linear functions and use their intercept as the position of the scattering shoulder.[83,120] An alternative approach to fitting the data, where the low-q upturn is fit simulatneously with with peak is considered in the discussion section.

V. DISCUSSION

A. Solution structure

The correlation length of a salt-free polyelectrolyte solution is predicted by the scaling theory to be:

$$\xi = \left(\frac{B}{bc}\right)^{1/2} \tag{5}$$

where b is the monomer length ($\simeq 5.15$ Å for cellulose polymers), B is the stretching parameter, which describes the extent of chain folding inside a correlation blob, and c is the number concentration of repeating units.[46] Each correlation blob contains g_ξ monomers:

$$g_\xi \simeq B\xi/b \tag{6}$$

The correlation length can be measured from the position of the peak or the shoulder in the scattering function (q^*) as:

$$\xi = 2\pi/q^* \tag{7}$$

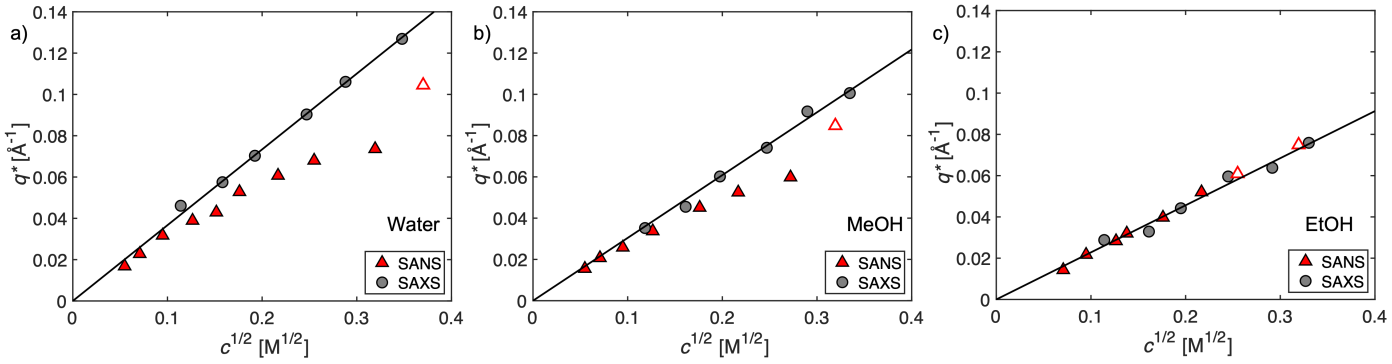

FIG. 5. Peak or shoulder positions (q^*) as determined from I vs. q curves (SANS: triangles, SAXS: circles) for TBACMC in a) Water ($\varepsilon \simeq 78$), b) Methanol ($\varepsilon \simeq 32$) and c) Ethanol ($\varepsilon \simeq 24$) as a function of concentration. Full symbols are for samples displaying a peak and hollow symbols are for samples displaying a shoulder. Lines are fits to SAXS data (water and MeOH) and to SANS and SAXS data (EtOH). The best-fit values of $B \simeq 0.85$ (water) $B \simeq 1.4$ (methanol) and $B \simeq 2.5$ (ethanol).

Decoupling of backbone and counterion fluctuations

The peak positions in the SANS and SAXS spectra of TBACMC in H_2O, MeOH and EtOH are plotted as a function of $c^{1/2}$ in Figures 5. For all three solvents, the SAXS peak positions, which approximately correspond to the maxima in $S(q)_{mm}$, follow a power-law of $q^* \propto c^{1/2}$, as expected by Eqs. 5 and 7. For H_2O and MeOH, the maxima in $S(q)_{cc}$, measured by SANS, agrees with $S(q)_{mm}$ measured by SAXS at low concentrations, but q^* at intermediate and high concentrations deviate to lower values. As before, we interpret this as resulting from a decoupling of the lengthscales over which the polymer backbone and the counterions fluctuate. This is not observed for solutions in ethanol, for which the values of q^* measured by SANS and SAXS agree over the entire concentration range. However, while the SAXS signal displays a clear peak over the entire concentration range studied, the SANS signal displays a shoulder for $c \gtrsim 0.05$ M. Therefore, even though both monomer and counterion fluctuations occur over a similar lengthscales the counterions appear to be less strongly correlated than the monomers for this system. For DMF solutions, SAXS data showed shoulders over the entire concentration range measured, while SANS data showed clear peaks except at the low concentrations. The reason for this behaviour remains unclear.

In an earlier study on aqueous CMC solutions,[83] we observed that concentration fluctuations between backbone and counterions decouple at high concentrations for tetra-alkylammonium salts of CMC but not for alkali salts. The decoupling was more pronounced for larger TAA salts. The fraction of dissociated counterions for both salts is nearly identical (see discussion below). The decoupling could then be assigned to the solvophobic nature of the TAA ions, but it seems counterintuitive that solvophobic ions should be more delocalised from the backbone, thereby maximising contacts with the solvent. In any case, if the counterion-solvent interactions play a role in delocalisation, the results in figure 5 could be assigned to differences in solvation of the TBA^+ ion by ethanol compared to water and MeOH. Alternatively, the higher fraction of condensed counterions for ethanol relative to water and methanol may oppose the decoupling of concentration fluctuations between monomers and counterions. SANS and SAXS data for TBAPSS in water show a much weaker decoupling than for TBACMC, presumably due to the higher fraction of condensed counterions.

The Stretching Parameter

To calculate the stretching parameter B for TBACMC, the q^* value of $S(q)_{mm}$ should be employed. In order to estimate this, we used the following approach: for H_2O, MeOH and EtOH, NMF and NMA the q^* values in the SAXS profiles, which are our best estimate for $S(q)_{mm}$ are used to calculate the correlation length. For methanol and water, plotting the stretching obtained from SANS and SAXS peaks as a function of concentration, it is observed that the values obtained from the two techniques converge at low polymer concentrations. We therefore use this method for DMSO and DMF, for which we lack SAXS measurements of the correlation length. The best-fit values of the stretching parameter are listed in table II.

The scaling theory models the conformation inside a correlation blob as a pole of electrostatic blobs of size ξ_{el}. Inside the electrostatic blob the conformation is unaffected by electrostatic interactions. On distances larger than ξ_{el}, electrostatic repulsion strongly stretches the chain. For flexible polymers, as the effective charge of the backbone decreases, the size of the electrostatic blob increases allowing for greater chain folding inside the correlation blob, which results in higher values of the stretching parameter.[130] For semiflexible chains, where the bare (intrinsic) Kuhn segment is much larger than ξ_{el}, chains cannot fold inside the electrostatic blob. The electrostatic blob size is predicted to be of the order of the Bjerrum length when there is more than one dissociated counterion per Kuhn segment.[17,46] In this case, the stretching parameter should be charge-independent and close to unity. Experimental results for semiflexible polyelectrolytes support this, as shown in figure 6. The correlation length of double stranded DNA and several polysaccharides follows a scaling law of $\xi \simeq (bc)^{-1/2}$, corresponding to Eq. 5 with $B = 1$.

Solvent	l_B [nm]	B	Λ(0.065M) [Scm^2]	λ_C [mScm^2/mol]	$\lambda_C\eta_s$ [10^{-2}NsS/mol]	f_{exp} [-]	f_{exp}/f_M [b] [-]
NMA ($T = 35$ °C)	0.31	1.27	3×10^{-3}	6.85 [e]	23.5	0.71	0.43
NMF	0.31	1.25	1.1×10^{-3}	14[f]	23.5	0.66	0.4
Water	0.71	$\simeq 1$[a]	4.0×10^{-3}	19.47	17.4	0.61	0.85
DMSO	1.19	(1.26)[b]	1.3×10^{-3}	9.23	23.2	0.34	0.78
EG	1.5	(2.5)[c]	1.6×10^{-4}	1.51	25.1	0.25	0.67
DMF	1.5	(1.7)[b]	1.2×10^{-4}	22.90	21.05	0.23	0.66
Methanol	1.71	1.4	6.1×10^{-4}	39.08	21.3	0.28	0.95
Ethanol	2.24	2.5	2.6×10^{-4}	19.74	21.4	0.15	0.65
1-propanol	2.72	$\simeq 2$[d]	-	11.0	21.42	-	-
1-butanol	3.2	-	-	7.84	21.05	-	-

TABLE II. Properties of TBACMC in various solvents. [a] Value for NaCMC. For TBACMC the best-fit SAXS results in ref. [83] give $B \simeq 0.85$, which is unphysical. Hou et al's measurements for TBACMC give $B \simeq 1$.[57] [b] Value estimate by linearly extrapolating B calculated from SANS data to $c = 0$, see the text. For DMF, the value calculated from the position of the SAXS shoulders is $B = 1.8$ [c] Average value from four SANS measurements. [d] none of the samples measured showed peaks, [e] calculated using data from refs.[121,122] assuming that the Walden product at 35 °C and 40 °C is the same. [f] from ref. [123]

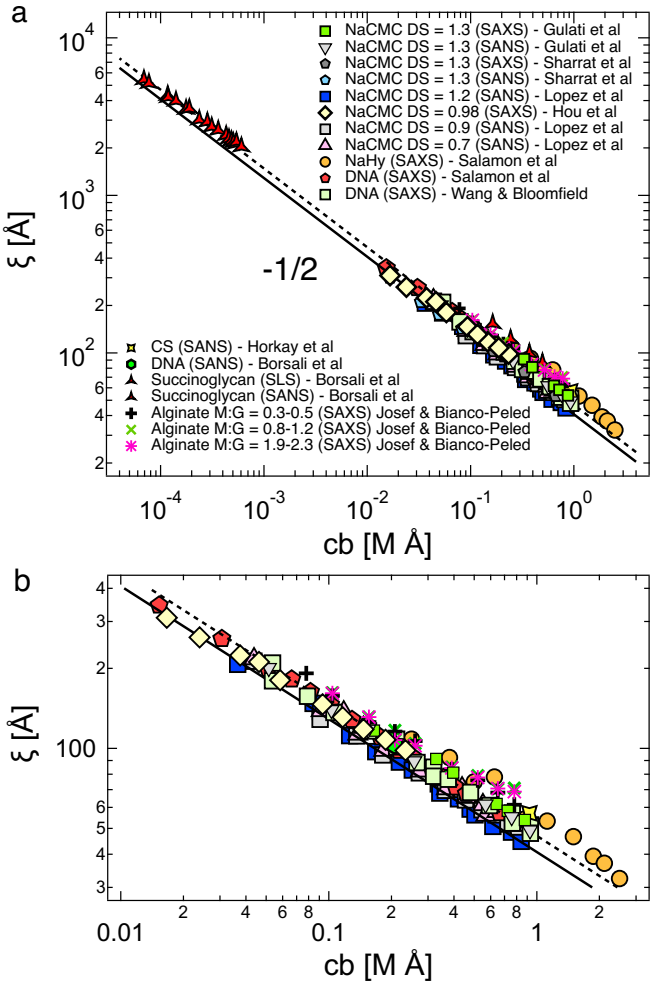

FIG. 6. Correlation length of semiflexible polyelectrolytes in salt-free water, data are from refs. [49,62,83,95,96,120,124–128], see legend. Part b zooms into the high concentration regime. Full line is scaling theory with $B = 1$ and dashed line is Koyama's prediction.[129] The monomer length is $b = 5.15$ Å for polysaccharides and 3.4 Å for double stranded DNA. CS is for chondroitin sulfate. M:G is the ratio of mannuronic acid to guluronic acid in alginate.[49]

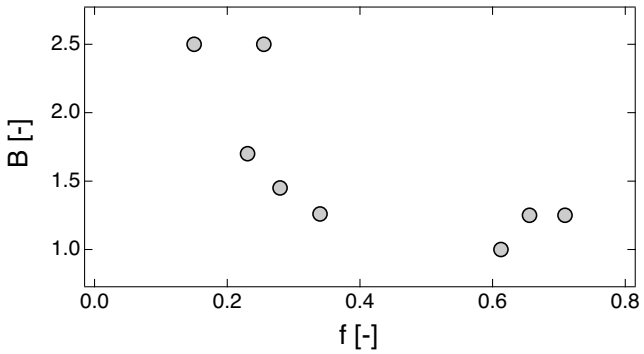

FIG. 7. Dependence of the stretching parameter on the effective charge of the CMC backbone. The values of f are calculated from conductivity and scattering data, as discussed in section V A.

Figure 7 plots the stretching parameter as a function of the fraction of monomers with a dissociated counterion, where f is obtained from conductivity as discussed below. For NMA, NMF, water and DMSO ($l_B \simeq 0.3 - 1.2$ nm) the stretching parameter B takes a value close to unity. For DMF, ethylene glycol methanol and ethanol, the higher values of B imply some degree of folding inside the correlation blobs. This result is only expected from the scaling model if the Kuhn segment is smaller than the electrostatic blob. For CMC, the intrinsic Kuhn length in water is $l_{K,0} \simeq 10$ nm.[131] Values of $l_{K,0}$ in other solvents have not been reported but it seems unlikely that it will be smaller than 1-2 nm as required for $l_K \lesssim \xi_{el}$. Alternatively, changes in B may not be related to the electrostatic blob size and instead reflect the solvent-dependent local conformation of the cellulose backbone. In this case, the correlation of B with f would be accidental.

Influence of solvent properties on peak sharpness

Figure 8 compares the SANS curves of TBACMC solutions at a concentration of $c = 0.033$ M in methanol, ethanol and 1-butanol. A clear peak is observed for the solution in methanol.

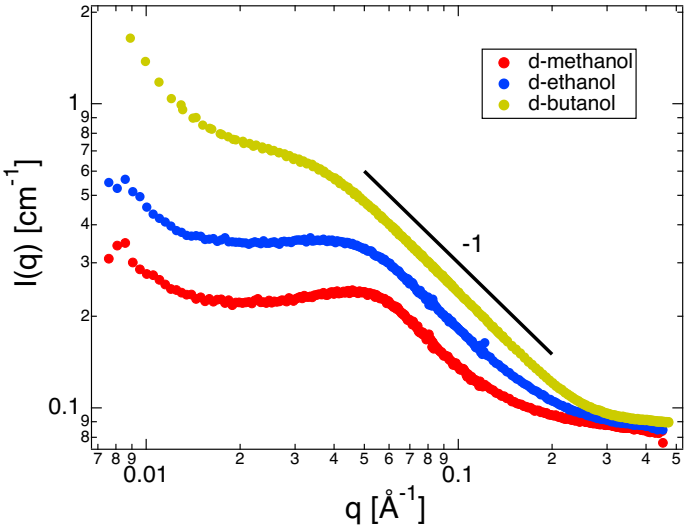

FIG. 8. SANS curves for $c = 0.033$ M solutions of TBACMC in three linear alcohols. Line is a power law with exponent of -1.

In ethanol a similar but broader peak is observed and the 1-butanol solution displays a shoulder feature. The scaling model explains the presence of the correlation peak in polyelectrolyte solutions as follows: the large osmotic pressure generated by free counterions suppresses long-ranged concentration fluctuations in polyelectrolyte solutions, generating a correlation hole at low q and the maximum in the structure factor of salt-free polyelectrolyte solutions. More specifically, the scaling theory predicts that, for solutions without added salt, the structure factor displays a peak if there is more than one dissociated charge per correlation blob. This appears to be inconsistent with the results reported here: in 1-propanol solutions, no peak is observed for concentrations as low as 0.014 M ($\xi \simeq 20$ nm, $g_\xi \simeq 90$). By contrast in methanol a peak is observed at $c = 0.11$ M ($\xi \simeq 6$ nm, $g_\xi \simeq 17$). This would imply that f for methanol should be $\simeq 5\times$ higher than in 1-propanol, which seems unreasonable given that the dielectric constant is only $\simeq 1.5\times$ lower.

The theory of Koyama[129] explains the peak as arising from the strong repulsion between like-charged polymer segments, which induces local ordering. Koyama's theory expects a peak for neutral polymer solutions if the repulsive interactions between chains is sufficiently strong. As the Bjerrum length of the solvent increases, the effective charge of the backbone decreases, which weakens electrostatic repulsions between like-charged segments. However, the Coulomb potential between two charges increases proportionally to the Bjerrum length. Therefore, it is not clear if the results in figure 8 can be accounted for by invoking Koyama's model.

A third possible explanation for the disappearance of the peak is the stronger low-q upturn. For the SAXS measurements, the contribution from the capillary background is too strong at low q, preventing us from resolving this upturn. In the SANS experiments, the measured q-range did not extend sufficiently far into the low-q regime to capture the upturn well. When we fit a power law to the low-q region and subtract this contribution from the total scattering signal (see figure 9), a peak becomes apparent, the of which position is usually not very different from that of obtained by fitting two power-laws to the unsubtracted signal . The appearance of the peak in the subtracted signal may simply be an artifact of the subtraction procedure. Data for aqueous solutions provide evidence against the low-q upturn being the cause of the peak disappearance. For aqueous solutions at modest concentrations, the low-q upturn is much stronger for NaCMC than for TBACMC, see fig. 5 of ref. [83], however NaCMC displays a clear correlation peak but TBACMC does not.

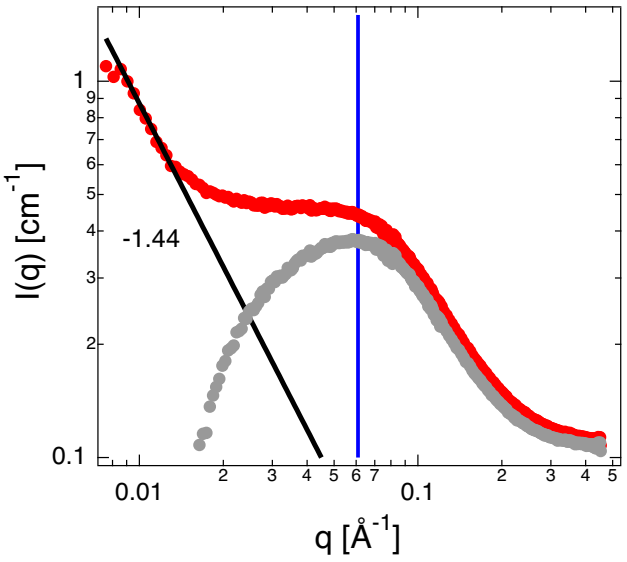

FIG. 9. Red points are the SANS intensity for a solution of TBACMC in deuterated ethanol at a concentration of 0.07 M. The black line is a power law fit to the low q data and the grey points are the measured intensity minus the power-law fit. The blue line indicates the position of the shoulder, obtained from fitting the total scattering intensity.

Figure 10 compares the SANS profiles of TBACMC at a concentration of $c = 0.11$ M in three solvents. The curve for DMSO displays a sharper peak than the one in water. In the case of ethanol no maximum in the scattering intensity is observed and only a broad shoulder is apparent, indicating a broader (less localised) distribution of counterions. As discussed above, the scaling theory expects peak sharpness to correlate with the charge density of the polymer, with higher charge densities resulting in sharper peaks, which is not observed here.

Comparison with behaviour of flexible polyelectrolytes

In two earlier studies on the scattering properties of flexible polyelectrolytes[20,132] we observed that for solvents of low dielectric constant, the scaling of the correlation length with concentration follows $\xi \propto c^{-1/3}$. We interpreted this as arising from the chain collapse onto a pearl-necklace structure. The collapse can be driven by solvophobic forces or attractive forces between condensed counterions. The results presented here show for CMC do not show any indication of polymer collapse and the scaling of $\xi \propto c^{-1/3}$ is

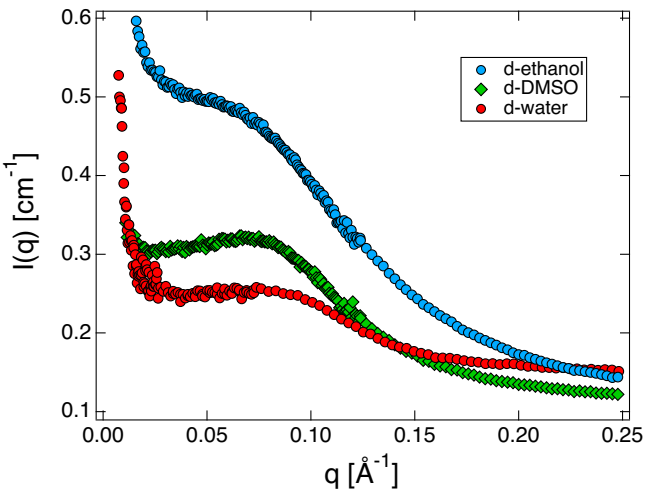

FIG. 10. SANS intensity I as a function of scattering wavevector q for TBACMC in water, DMSO and EtOH at 0.11 M with an observable difference in correlation peak sharpness.

never observed. One possible reason is that for our polymer, there is one charged group per 0.4 nm, compared to $\simeq 1$ per 0.25 nm[133] for polystyrene sulfonate and poly(1-butyl-3-vinylimidazolium bis(trifluoromethanesulfonyl)imide). This should result in a lower density of condensed counterions and correspondingly weaker counterion-induced attraction. Additionally, the semiflexible nature of the CMC backbone likely prevents the local collapse of chains into globules.

B. Counterion condensation

The theory of Colby et al relates the fraction of charged monomers (f) to the specific conductance (Λ) of semidilute,[134] salt-free polyelectrolyte solution as:[94]

$$\Lambda = f\left[\lambda_C + \frac{fe^2c\xi^2N_A^2ln(\xi/D)}{3\pi\eta_s}\right] \qquad (8)$$

where λ_C is the limiting specific conductance of the counterion in the solvents, D is the cross-sectional diameter of the chain, taken to be 3.5 Å for in all solvents, N_A is the Avogadro constant, c is the concentration of repeating units per unit volume and e is the unit of charge. The specific conductances for the TBA ion in various solvents are listed in table II.

Figure 11 plots the fraction of monomers bearing a dissociated charge (f) as a function of polymer concentration for NaCMC and TBACMC. Despite the differences in size and affinity for water for Na^+ and TBA^+, the calculated value of f differ by less than 10%. This reinforces previous findings that while counterion valence has a large influence on polyelectrolyte properties, changing the ion type for a given valence has a much weaker effect.[135–137] The slight increase of f at high concentrations is consistent with earlier measurements on NaCMC of various degrees of substitution and also with conductivity and osmotic pressure data of polystyrene sulfonate solutions.[85]

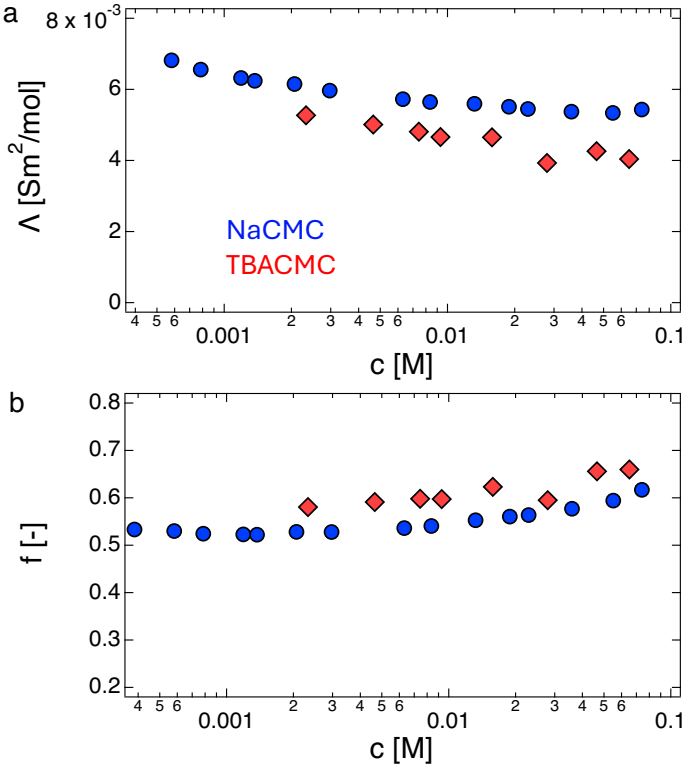

FIG. 11. Comparison of conductance (a) and fraction of monomers bearing a dissociated counterion (b) for semidilute solutions of NaCMC and TBACMC as a function of polymer concentration. The values of f are calculated using Eq. 8 with $B = 1$ for both salts.

Figure 12a plots the fraction of charged monomers as a function of polymer concentration for TBACMC in different solvents. We use the values of B listed in table II to calculate the correlation length and fix $D = 7$ Å for all solvents.[95] With these values, equation 8 is used to calculate f for each polymer concentration.

A test for the applicability of the Oosawa-Manning model to semidilute TBACMC solutions is provided in fig 12b, where the inverse of the fraction of monomers with a dissociated counterion is plotted as a function of l_B. A linear relationship between these two quantities, as expected by Eq. 1 theory is observed, but the effective charge density corresponds to approximately one charge per $1.3l_B$, shown by the dashed black line. These results are in line with earlier studies on the conductivity of NaCMC in water,[80,81,91] which also found charge densities lower than expected by the OM model. Water, NMA and NMF show $f \simeq 0.65$ despite having different dielectric constants. Equation 1 only expects f to be independent of the Bjerrum length when all counterions are dissociated. The reason for this discrepancy is not clear to us presently.

In an earlier study, we concluded that for NaCMC in water, Eq. 8 likely underestimates the fraction of dissociated counterions because it assumes that the dissociated counterion mobility is equal to that of the free ion.[80] The actual fraction of free counterions may therefore be somewhat close to Eq. 1 than the values shown in figure 12.

The red line in figure 12 is calculated assuming a monomer

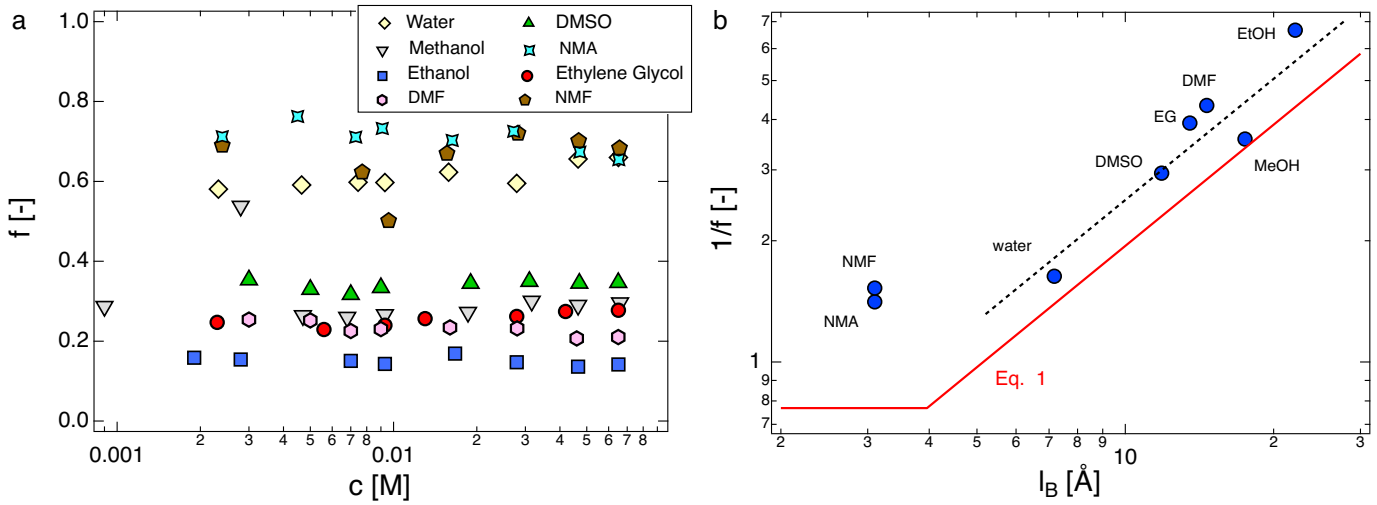

FIG. 12. a) Fraction of monomers with a dissociated counterion (f) as a function of polymer concentration for TBACMC solutions. f is calculated using Eq. 8. b) reciprocal of the fraction of monomers with a dissociated counterion as a function of Bjerrum length (l_B). Values of f are an average over all concentrations in part a. The red line is Eq. 1 with $n = \mathrm{DS} = 1.3$ and $b = 5.15$ Å. Note that $f^{-1} \simeq 0.77$ is predicted in the low l_B limit, corresponding to 1.3 dissociated counterions per monomer. The dashed line, which lies 30% above the red line, corresponds to the best-fit line for $l_B > 5$ Å.

size of $b = 5.15$ Å. However, as discussed above, the stretching parameter data suggest that the effective monomer size may be lower in some solvents. The question then arises of whether using $b = 5.15$ Å gives the correct distance between charges. In order to answer this, it would be necessary to know whether folding of the CMC chain occurs on length-scales smaller or larger than the distance between charges, but we lack such information.

VI. CONCLUSIONS

Our results demonstrate a clear dependence of the effective charge fraction on the solvent dielectric constant. At fixed polymer concentration, the fraction of dissociated monomers, f, scales approximately with the inverse Bjerrum length, in qualitative agreement with the Oosawa-Manning condensation model. However, differences in f for solvents of similar dielectric constants suggest that continuum electrostatics alone may not fully explain counterion condensation.

The stretching parameter B, extracted from small angle scattering measurements was found to be solvent dependent. High-permittivity solvents such as NMA, NMF, water, and DMSO yield B values close to unity, consistent with semi-flexible chains which are fully stretched inside the correlation blobs. This value is consistent with literature results for semiflexible polyelectrolytes including DNA and several polysaccharides. Lower-permittivity solvents such as methanol, ethanol, and DMF exhibit larger B values, suggesting partial folding within the correlation blob, but the origin of this effect remains unclear. At present, it is not known whether the higher values of the stretching parameter reflect solvent-driven changes in the intrinsic (non-electrostatic) conformation of the cellulose backbone or if electrostatic stretching plays a role.

The scattering data reveal solvent-dependent coupling between polymer backbone and counterion concentration fluctuations. In water and methanol, SANS and SAXS peak positions coincide at low concentrations but diverge at higher concentrations, suggesting a decoupling of counterion and monomer fluctuations. In ethanol, the peak positions measured by the two techniques remains equal across the entire concentration range. This suggests that decoupling occurs if f is sufficiently high and/or the counterions are sufficiently solvophobic, but more data are needed to confirm this point.

ACKNOWLEDGEMENTS

We thank the ILL (10.5291/ILL-DATA.9-11-1961) and the SPring-8 synchrotron radiation facility (Hyogo, Japan) for beamtime at BL40B2 (Proposal number: 2024A1203). We thank Noboru Ohta for help with the SAXS experiments. Hannes Luhmann (RWTH) and the students of the Watanabe group at Okayama university (Rene Iwato, Yume Tao, and Hikari Tsunekawa) are thanked for their help running the SAXS measurements. The authors acknowledge funding from the DFG (project: GO 3250/2-1) and the JSPS KAKENHI projects (JP24K01236 and JP20KK0325). We thank prof. Atsushi Matsumoto (University of Fukui) for help with the scattering experiments and for providing us with N-methylformamide. We thank Ralph H. Colby for useful comments on the manuscript.

CONFLICT OF INTEREST

The authors declare no conflict of interest.

REFERENCES

[1] A. V. Dobrynin and M. Rubinstein, "Theory of polyelectrolytes in solutions and at surfaces," Progress in polymer science **30**, 1049–1118 (2005).

[2] R. Sayko, Y. Tian, H. Liang, and A. V. Dobrynin, "Charged polymers: From polyelectrolyte solutions to polyelectrolyte complexes," Macromolecules **54**, 7183–7192 (2021).

[3] A. Matsumoto, "Rheology of polyelectrolyte solutions: current understanding and perspectives," Nihon Reoroji Gakkaishi **50**, 43–50 (2022).

[4] A. Matsumoto, "Solution rheology of poly (ionic liquid) s: current understanding and open questions," Korea-Australia Rheology Journal **36**, 319–328 (2024).

[5] A. Traeger and M. N. Leiske, "The whole is greater than the sum of its parts–challenges and perspectives in polyelectrolytes," Biomacromolecules **26**, 5–32 (2024).

[6] B. H. Vilsinski, A. C. de Oliveira, P. R. Souza, and A. F. Martins, "Polysaccharide-based polyelectrolyte multilayers fabricated via layer-by-layer approach: From preparation to applications," Progress in organic coatings **196**, 108720 (2024).

[7] B. Sim, J. J. Chang, Q. Lin, J. H. M. Wong, V. Ow, Y. Leow, Y. J. Wong, Y. J. Boo, R. Goh, and X. J. Loh, "Hydrogels based on polyelectrolyte complexes: underlying principles and biomedical applications," Biomacromolecules **25**, 7563–7580 (2024).

[8] J. Li, L. Li, H. Brink, G. Allegri, and S. Lindhoud, "Polyelectrolyte complex-based materials for separations, progress, challenges and opportunities," Materials Horizons (2025).

[9] V. Baddam and H. Tenhu, "Thermoresponsive polycations," Polymer Chemistry **14**, 3647–3678 (2023).

[10] A. Tagliabue and M. Mella, "The role of counterion size in defining star-shaped polyelectrolytes thermodynamics, conformations, and ion dynamics," Journal of Polymer Science (2025).

[11] M. Rubinstein and G. A. Papoian, "Polyelectrolytes in biology and soft matter," Soft Matter **8**, 9265–9267 (2012).

[12] M. Mussel, P. J. Basser, and F. Horkay, "Ion-induced volume transition in gels and its role in biology," Gels **7**, 20 (2021).

[13] F. Horkay, "Polyelectrolyte gels: a unique class of soft materials," Gels **7**, 102 (2021).

[14] F. Horkay, P. J. Basser, and E. Geissler, "Cartilage extracellular matrix polymers: hierarchical structure, osmotic properties, and function," Soft Matter **20**, 6033–6043 (2024).

[15] F. Horkay and P. J. Basser, "Organization of hyaluronic acid molecules in solutions," MRS advances **9**, 537–542 (2024).

[16] M. Muthukumar, *Physics of Charged Macromolecules* (Cambridge University Press, 2023).

[17] C. G. Lopez, A. Matsumoto, and A. Q. Shen, "Dilute polyelectrolyte solutions: recent progress and open questions," Soft Matter **20**, 2635–2687 (2024).

[18] M. Beer, M. Schmidt, and M. Muthukumar, "The electrostatic expansion of linear polyelectrolytes: Effects of gegenions, co-ions, and hydrophobicity," Macromolecules **30**, 8375–8385 (1997).

[19] A. Matsumoto, R. Ukai, H. Osada, S. Sugihara, and Y. Maeda, "Tuning the solution viscosity of ionic-liquid-based polyelectrolytes with solvent dielectric constants via the counterion condensation," Macromolecules **55**, 10600–10606 (2022).

[20] A. Gulati, L. Meng, T. Watanabe, and C. G. Lopez, "Electrostatically-driven collapse of polyelectrolytes: The role of the solvent's dielectric constant," Journal of Polymer Science (2025), https://doi.org/10.1002/pol.20250574.

[21] A. Chremos and J. F. Douglas, "Polyelectrolyte association and solvation," The Journal of chemical physics **149** (2018).

[22] A. Chremos and J. F. Douglas, "Communication: When does a branched polymer become a particle?" The Journal of Chemical Physics **143** (2015).

[23] A. Gavrilov, A. Chertovich, and E. Y. Kramarenko, "Conformational behavior of a single polyelectrolyte chain with bulky counterions," Macromolecules **49**, 1103–1110 (2016).

[24] Y. D. Gordievskaya, A. A. Gavrilov, and E. Y. Kramarenko, "Effect of counterion excluded volume on the conformational behavior of polyelectrolyte chains," Soft Matter **14**, 1474–1481 (2018).

[25] S. Kondou, Y. Sakashita, A. Morinaga, Y. Katayama, K. Dokko, M. Watanabe, and K. Ueno, "Concentrated nonaqueous polyelectrolyte solutions: high na-ion transference number and surface-tethered polyanion layer for sodium-metal batteries," ACS Applied Materials & Interfaces **15**, 11741–11755 (2023).

[26] X. Gao, K. Yamamoto, T. Hirai, N. Ohta, T. Uchiyama, T. Watanabe, H. Imai, S. Sugawara, K. Shinohara, and Y. Uchimoto, "Impact of the composition of alcohol/water dispersion on the proton transport and morphology of cast perfluorinated sulfonic acid ionomer thin films," ACS omega **6**, 14130–14137 (2021).

[27] Y. Qiu, X. Zhao, H. Li, S. Liu, and W. Yu, "Microstructures and rheological properties of short-side-chain perfluorosulfonic acid in water/2-propanol," Polymers **16**, 1863 (2024).

[28] S. Wang, J. Song, W. Zhao, P. Guan, M. Li, M. Zhang, Y. Zou, J. Liu, G. Chen, H. Ren, *et al.*, "Nanostructures and multi-scale aggregation of high ion exchange capacity short-side-chain perfluorosulfonic acid dispersion," Journal of Colloid and Interface Science **672**, 805–813 (2024).

[29] J. Shin, H. Shin, S.-H. Lee, J. D. Jang, and H. J. Kim, "Influence of solvent dielectric constant on the complex coacervation phase behavior of polymerized ionic liquids," ACS Macro Letters **13**, 1678–1685 (2024).

[30] M. Novy, D. Duchesne, G. Dahlke, L. P. Chen, and R. B. Moore, "Effect of ionomer–solvent interactions in pfsa dispersions: Dispersion morphology," Macromolecules **58**, 8854–8865 (2025).

[31] F. Oosawa, "A simple theory of thermodynamic properties of polyelectrolyte solutions," Journal of Polymer Science **23**, 421–430 (1957).

[32] G. S. Manning, "Limiting laws and counterion condensation in polyelectrolyte solutions i. colligative properties," The journal of chemical Physics **51**, 924–933 (1969).

[33] G. S. Manning, "The molecular theory of polyelectrolyte solutions with applications to the electrostatic properties of polynucleotides," Quarterly reviews of biophysics **11**, 179–246 (1978).

[34] G. Chen, A. Perazzo, and H. A. Stone, "Electrostatics, conformation, and rheology of unentangled semidilute polyelectrolyte solutions," Journal of Rheology **65**, 507–526 (2021).

[35] N. Marioni, A. Rajesh, Z. Zhang, B. D. Freeman, and V. Ganesan, "What is the influence of ion aggregation and counterion condensation on salt transport in ion exchange membranes?" Journal of Membrane Science **701**, 122713 (2024).

[36] C. Wandrey, "Concentration regimes in polyelectrolyte solutions," Langmuir **15**, 4069–4075 (1999).

[37] C. Wandrey, D. Hunkeler, U. Wendler, and W. Jaeger, "Counterion activity of highly charged strong polyelectrolytes," Macromolecules **33**, 7136–7143 (2000).

[38] Q. Liao, A. V. Dobrynin, and M. Rubinstein, "Molecular dynamics simulations of polyelectrolyte solutions: osmotic coefficient and counterion condensation," Macromolecules **36**, 3399–3410 (2003).

[39] R. M. Nyquist, B.-Y. Ha, and A. J. Liu, "Counterion condensation in solutions of rigid polyelectrolytes," Macromolecules **32**, 3481–3487 (1999).

[40] M. Muthukumar, "Theory of counter-ion condensation on flexible polyelectrolytes: Adsorption mechanism," The Journal of chemical physics **120**, 9343–9350 (2004).

[41] A. Kundagrami and M. Muthukumar, "Theory of competitive counterion adsorption on flexible polyelectrolytes: Divalent salts," The Journal of chemical physics **128** (2008).

[42] R. Kumar, A. Kundagrami, and M. Muthukumar, "Counterion adsorption on flexible polyelectrolytes: comparison of theories," Macromolecules **42**, 1370–1379 (2009).

[43] This is in contrast to the scaling model, which expects the conformation of a polylectrolyte chain to be independent of the effective charge fraction if the Bjerrum length is smaller than the intrinsic Kuhn segment of the polymer.

[44] S. Dou and R. H. Colby, "Charge density effects in salt-free polyelectrolyte solution rheology," Journal of Polymer Science Part B: Polymer Physics **44**, 2001–2013 (2006).

[45] M. Kowblansky and P. Zema, "Interactions of sodium ions with the sodium salts of poly (acrylic acid/acrylamide) copolymers of varying charge density," Macromolecules **14**, 166–170 (1981).

[46] A. V. Dobrynin, R. H. Colby, and M. Rubinstein, "Scaling theory of polyelectrolyte solutions," Macromolecules **28**, 1859–1871 (1995).

[47] S. Jousset, H. Bellissent, and J. C. Galin, "Polyelectrolytes of high charge density in organic solvents. synthesis and viscosimetric behavior," Macromolecules **31**, 4520–4530 (1998).

[48] M. Lee, S. L. Perry, and R. C. Hayward, "Complex coacervation of polymerized ionic liquids in non-aqueous solvents," ACS Polymers Au **1**, 100–106 (2021).

[49] C. Hou, T. Watanabe, C. G. Lopez, and W. Richtering, "Structure and rheology of carboxymethylcellulose in polar solvent mixtures," Carbohydrate Polymers **347**, 122287 (2025).

[50] R. Marcilla, J. Alberto Blazquez, J. Rodriguez, J. A. Pomposo, and D. Mecerreyes, "Tuning the solubility of polymerized ionic liquids by simple anion-exchange reactions," Journal of Polymer Science Part A: Polymer Chemistry **42**, 208–212 (2004).

[51] T. Ono, T. Sugimoto, S. Shinkai, and K. Sada, "Lipophilic polyelectrolyte gels as super-absorbent polymers for nonpolar organic solvents," Nature materials **6**, 429–433 (2007).

[52] T. Ono, T. Sugimoto, S. Shinkai, and K. Sada, "Molecular design of superabsorbent polymers for organic solvents by crosslinked lipophilic polyelectrolytes," Advanced Functional Materials **18**, 3936–3940 (2008).

[53] T. Ono, M. Ohta, K. Iseda, and K. Sada, "Counter anion dependent swelling behaviour of poly (octadecyl acrylate)-based lipophilic polyelectrolyte gels as superabsorbent polymers for organic solvents," Soft Matter **8**, 3700–3704 (2012).

[54] T. Ono, M. Ohta, and K. Sada, "Ionic polymers act as polyelectrolytes in nonpolar media," ACS Macro Letters **1**, 1270–1273 (2012).

[55] J. Chen, S. Wang, J. Peng, J. Li, and M. Zhai, "New lipophilic polyelectrolyte gels containing quaternary ammonium salt with superabsorbent capacity for organic solvents," ACS Applied Materials & Interfaces **6**, 14894–14902 (2014).

[56] A. Gulati and C. G. Lopez, "Viscosity of polyelectrolytes: Influence of counterion and solvent type," ACS Macro Letters **13**, 1079–1083 (2024).

[57] C. Hou, W. Richtering, T. Watanabe, K. Leonhard, M. Papusha, and C. G. Lopez, "Solutions of carboxymethylcellulose with organic counterions (i): The influence of counterion properties on the polymer structure and solubility," Macromolecules **58**, 7489–7499 (2025).

[58] R. L. Feddersen and S. N. Thorp, "Sodium carboxymethylcellulose," in *Industrial gums* (Elsevier, 1993) pp. 537–578.

[59] V. Stigsson, D. I. Wilson, and U. Germgärrd, "Production variance in purified carboxymethyl cellulose (cmc) manufacture," Developments in Chemical Engineering and Mineral Processing **12**, 217–231 (2004).

[60] V. Stigsson, G. Kloow, and U. Germgård, "An historic overview of carboxymethyl cellulose (cmc) production on an industrial scale," PaperAsia **17** (2001).

[61] C. Barba, D. Montané, M. Rinaudo, and X. Farriol, "Synthesis and characterization of carboxymethylcelluloses (cmc) from non-wood fibers i. accessibility of cellulose fibers and cmc synthesis," Cellulose **9**, 319–326 (2002).

[62] C. G. Lopez, R. H. Colby, and J. T. Cabral, "Electrostatic and hydrophobic interactions in nacmc aqueous solutions: Effect of degree of substitution," Macromolecules **51**, 3165–3175 (2018).

[63] C. G. Lopez and W. Richtering, "Oscillatory rheology of carboxymethyl cellulose gels: Influence of concentration and ph," Carbohydrate polymers **267**, 118117 (2021).

[64] M. S. Rahman, M. S. Hasan, A. S. Nitai, S. Nam, A. K. Karmakar, M. S. Ahsan, M. J. Shiddiky, and M. B. Ahmed, "Recent developments of carboxymethyl cellulose," Polymers **13**, 1345 (2021).

[65] R. Ramakrishnan, J. T. Kim, S. Roy, and A. Jayakumar, "Recent advances in carboxymethyl cellulose-based active and intelligent packaging materials: A comprehensive review," International Journal of Biological Macromolecules **259**, 129194 (2024).

[66] A. Zennifer, P. Senthilvelan, S. Sethuraman, and D. Sundaramurthi, "Key advances of carboxymethyl cellulose in tissue engineering & 3d bioprinting applications," Carbohydrate polymers **256**, 117561 (2021).

[67] M. Rinaudo, J. Mazet, and M. Milas, "Propriétés thermodynamiques des polyanions à densité de charge variable," CR Acad. Sci. , 1401–1404 (1973).

[68] M. Rinaudo, L. B, and M. Milas, "Determination of dissociation constant of polyacids by potentiometry," COMPTES RENDUS HEBDOMADAIRES DES SEANCES DE L ACADEMIE DES SCIENCES SERIE C **273**, 1148 (1971).

[69] M. Rinaudo and M. Milas, "Interaction of monovalent and divalent counterions with some carboxylic polysaccharides," Journal of Polymer Science: Polymer Chemistry Edition **12**, 2073–2081 (1974).

[70] M. Rinaudo and M. Mils, "Polyelectroyte behavior of a bacterial polysaccharide from xanthomonas campestris: Comparison with carboxymethylcellulose," Biopolymers: Original Research on Biomolecules **17**, 2663–2678 (1978).

[71] M. Rinaudo, "Polyelektrolyteigenschaften von carboxymethylcellulose in wäbriger lösung. einflub der ladungsdichte," Faserforsch. Textiltech. , 21–28 (1973).

[72] M. Rinaudo and M. Milas, "Ionic selectivity of polyelectrolytes in salt free solutions," in *Polyelectrolytes and their Applications* (Springer, 1975) pp. 31–49.

[73] M. Nagasawa and I. Kagawa, "Colligative properties of polyelectrolyte solutions. iv. activity coefficient of sodium ion," Journal of Polymer Science **25**, 61–76 (1957).

[74] M. Rinaudo and C. Pierre, "Volume spécifique partiel des polyélectrolytes," CR Acad. Sci. , 1280 (1969).

[75] M. Rinaudo and M. Milas, "Propriétés électrochimiques des polyélectrolytes à densité de charge élevée," Journal de Chimie Physique **66**, 1489–1496 (1969).

[76] R. Zana, C. Tondre, M. Rinaudo, and M. Milas, "Étude ultrasonore de la fixation sur site des ions alcalins sur des carboxymethylcelluloses de densité de charge variable," Journal de Chimie Physique **68**, 1258–1266 (1971).

[77] C. Tondre and R. Zana, "Ultrasonic absorption as a probe for the study of site binding of counterions in polyelectrolyte solutions," The Journal of Physical Chemistry **75**, 3367–3372 (1971).

[78] C. Tondre and R. Zana, "Apparent molal volumes of polyelectrolytes in aqueous solutions," The Journal of Physical Chemistry **76**, 3451–3459 (1972).

[79] R. Zana, "Studies of aqueous solutions of polyelectrolytes by means of ultrasonic methods," Journal of Macromolecular Science—Reviews in Macromolecular Chemistry **12**, 165–189 (1975).

[80] E. Abbasi GharehTapeh, T. Watanabe, F. Horkay, C. Hou, C. Lopez, and M. Hohenschutz, "Counterion condensation, ion pairing and scattering properties of carboxymethyl cellulose with mono- and di-valent ions," Cellulose, submitted.

[81] D. Truzzolillo, F. Bordi, C. Cametti, and S. Sennato, "Counterion condensation of differently flexible polyelectrolytes in aqueous solutions in the dilute and semidilute regime," Physical Review E—Statistical, Nonlinear, and Soft Matter Physics **79**, 011804 (2009).

[82] D. Truzzolillo, C. Cametti, and S. Sennato, "Dielectric properties of differently flexible polyions: a scaling approach," Physical Chemistry Chemical Physics **11**, 1780–1786 (2009).

[83] A. Gulati, J. F. Douglas, O. Matsarskaia, and C. G. Lopez, "Influence of counterion type on the scattering of a semiflexible polyelectrolyte," Soft matter **20**, 8610–8620 (2024).

[84] J. Combet, F. Isel, M. Rawiso, and F. Boué, "Scattering functions of flexible polyelectrolytes in the presence of mixed valence counterions: condensation and scaling," Macromolecules **38**, 7456–7469 (2005).

[85] F. Bordi, C. Cametti, and R. Colby, "Dielectric spectroscopy and conductivity of polyelectrolyte solutions," Journal of Physics: Condensed Matter **16**, R1423 (2004).

[86] P. Nandi and B. Das, "Effects of concentration, relative permittivity, and temperature on the solution behavior of sodium carboxymethylcellulose as probed by electrical conductivity," The Journal of Physical Chemistry B **109**, 3238–3242 (2005).

[87] P. Nandi, *Solution Properties of Sodium Carboxymethylcellulose in Acetonitrile -Water Mixed Solvent Media*, Ph.D. thesis (2009).

[88] P. Nandi and B. Das, "Electrical conductances of sodium carboxymethylcellulose in acetonitrile (1)+ water (2) mixed solvent media in the presence of sodium chloride at 308.15 k," Journal of Chemical & Engineering Data **56**, 2870–2876 (2011).

[89] A. Chatterjee, B. Das, and C. Das, "Polyion–counterion interaction behavior for sodium carboxymethylcellulose in methanol–water mixed solvent media," Carbohydrate polymers **87**, 1144–1152 (2012).

[90] R. Sharma, C. Das, S. Dahal, and B. Das, "Polyion–counterion interactions in sodium carboxymethylcellulose–ethylene glycol–water ternary solutions," Carbohydrate polymers **92**, 1546–1554 (2013).

[91] D. Ray, R. De, and B. Das, "Thermodynamic, transport and frictional properties in semidilute aqueous sodium carboxymethylcellulose solution," The Journal of Chemical Thermodynamics **101**, 227–235 (2016).

[92] B. Das and A. Chatterjee, "Salt-induced counterion condensation and related phenomena in sodium carboxymethylcellulose–sodium halide–methanol–water quaternary systems," Soft Matter **11**, 4133–4140 (2015).

[93] C. Das, B. Sharma, and B. Das, "Studies on counterion-condensation in sodium carboxymethylcellulose-2-butoxyethanol-water ternaries using electrical conductivity," Journal of Molecular Liquids **219**, 104–110 (2016).

[94] R. H. Colby, D. C. Boris, W. E. Krause, and J. S. Tan, "Polyelectrolyte conductivity," Journal of Polymer Science Part B: Polymer Physics **35**, 2951–2960 (1997).

[95] C. G. Lopez, S. E. Rogers, R. H. Colby, P. Graham, and J. T. Cabral, "Structure of sodium carboxymethyl cellulose aqueous solutions: A sans and rheology study," Journal of Polymer Science Part B: Polymer Physics **53**, 492–501 (2015).

[96] W. N. Sharratt, R. O'Connell, S. E. Rogers, C. G. Lopez, and J. T. Cabral, "Conformation and phase behavior of sodium carboxymethyl cellulose in the presence of mono-and divalent salts," Macromolecules **53**, 1451–1463 (2020).

[97] P.-G. De Gennes, P. Pincus, R. Velasco, and F. Brochard, "Remarks on polyelectrolyte conformation," Journal de physique **37**, 1461–1473 (1976).

[98] C. G. Lopez, R. H. Colby, P. Graham, and J. T. Cabral, "Viscosity and scaling of semiflexible polyelectrolyte nacmc in aqueous salt solutions," Macromolecules **50**, 332–338 (2017).

[99] L. N. Jimenez, C. D. Martinez Narvaez, and V. Sharma, "Solvent properties influence the rheology and pinching dynamics of polyelectrolyte solutions thickening the pot with glycerol and cellulose gum," Macromolecules **55**, 8117–8132 (2022).

[100] P. Wagner, S. Różańska, E. Warmbier, A. Frankiewicz, and J. Różański, "Rheological properties of sodium carboxymethylcellulose solutions in dihydroxy alcohol/water mixtures," Materials **16**, 418 (2023).

[101] P. Komorowska, S. Różańska, and J. Różański, "Effect of the degree of substitution on the rheology of sodium carboxymethylcellulose solutions in propylene glycol/water mixtures," Cellulose **24**, 4151–4162 (2017).

[102] S. Różańska, K. Verbeke, J. Różański, C. Clasen, and P. Wagner, "Capillary breakup extensional rheometry of sodium carboxymethylcellulose solutions in water and propylene glycol/water mixtures," Journal of Polymer Science Part B: Polymer Physics **57**, 1537–1547 (2019).

[103] D. R. Lide, *CRC handbook of chemistry and physics: a ready-reference book of chemical and physical data* (CRC press, 1995).

[104] K.-J. Han, J.-H. Oh, S.-J. Park, and J. Gmehling, "Excess molar volumes and viscosity deviations for the ternary system n, n-dimethylformamide+ n-methylformamide+ water and the binary subsystems at 298.15 k," Journal of Chemical & Engineering Data **50**, 1951–1955 (2005).

[105] K. Kassapidou, W. Jesse, M. Kuil, A. Lapp, S. Egelhaaf, and J. Van der Maarel, "Structure and charge distribution in dna and poly (styrenesulfonate) aqueous solutions," Macromolecules **30**, 2671–2684 (1997).

[106] J. Van der Maarel, L. Groot, J. Hollander, W. Jesse, M. Kuil, J. Leyte, L. Leyte-Zuiderweg, M. Mandel, and J. Cotton, "On the charge distribution in aqueous poly (styrenesulfonic acid) solutions. a small-angle neutron scattering study," Macromolecules **26**, 7295–7299 (1993).

[107] "https://www.ncnr.nist.gov/resources/n-lengths/," .

[108] Y. Marcus, "Tetraalkylammonium ions in aqueous and non-aqueous solutions," Journal of Solution Chemistry **37**, 1071–1098 (2008).

[109] A. Sehgal and T. A. Seery, "Polyelectrolyte self-diffusion: Fluorescence recovery after photobleaching of sodium poly (styrenesulfonate) in n-methylformamide," Macromolecules **36**, 10056–10062 (2003).

[110] S. Dou, *Synthesis and characterization of ion-containing polymers*, Ph.D. thesis (2007).

[111] S. Dou and R. H. Colby, "Solution rheology of a strongly charged polyelectrolyte in good solvent," Macromolecules **41**, 6505–6510 (2008).

[112] J. Cohen, Z. Priel, and Y. Rabin, "Viscosity of dilute polyelectrolyte solutions," The Journal of chemical physics **88**, 7111–7116 (1988).

[113] "Exception to this are the H^+ and OH^- ions, which have higher mobilities and as result conduct more than alkali metal or halide ions." ().

[114] H. Vink, "Electrolytic conductivity of polyeiectrolyte solutions," Die Makromolekulare Chemie: Macromolecular Chemistry and Physics **183**, 2273–2283 (1982).

[115] Viscosity data for TBAPSS in this same solvent**?** also suggest a high residual salt content. We do not have a way to explain why this is the case at present because the presence of any ionic component is expected to show up in the solution conductivity.

[116] G. Smolyakov, J.-M. Catala, N. Kutsevol, and M. Rawiso, "Influence of the nature of counterions and solvent on the structure of pss solutions," in *Modern Problems of Molecular Physics: Selected Reviews from the 7th International Conference Physics of Liquid Matter: Modern Problems, Kyiv, Ukraine, May 27-31, 2016* (Springer, 2017) pp. 133–147.

[117] M. Spiteri, "Conformation and arrangement of polyelectrolytes in semidiluted solution. a study by small angle neutrons scattering; conformation et arrangement des polyelectrolytes en solution semi-diluee. etude par diffusion des neutrons aux petits angles," (1997).

[118] K. Nishida, K. Kaji, T. Kanaya, and T. Shibano, "Added salt effect on the intermolecular correlation in flexible polyelectrolyte solutions: Small-angle scattering study," Macromolecules **35**, 4084–4089 (2002).

[119] "We assume $f = 0.5$ for CMC and $f = 0.3$ for napss following refs. 80,85," ().

[120] K. Salamon, D. Aumiler, G. Pabst, and T. Vuletic, "Probing the mesh formed by the semirigid polyelectrolytes," Macromolecules **46**, 1107–1118 (2013).

[121] L. R. Dawson, E. D. Wilhoit, R. R. Holmes, and P. G. Sears, "Solvents having high dielectric constants. v. limiting ionic equivalent conductances in n-methylacetamide at 40° 1, 2," Journal of the American Chemical Society **79**, 3004–3006 (1957).

[122] W. D. Williams, J. A. Ellard, and L. R. Dawson, "Solvents having high dielectric constants. vi. diffusion in n-methylacetamide1, 2," Journal of the American Chemical Society **79**, 4652–4654 (1957).

[123] N. G. Tsierkezos and A. I. Philippopoulos, "Studies of ion solvation and ion association of n-tetrabutylammonium hexafluorophosphate and n-tetrabutylammonium tetraphenylborate in various solvents," Fluid Phase Equilibria **277**, 20–28 (2009).

[124] F. Horkay, P. J. Basser, A.-M. Hecht, and E. Geissler, "Chondroitin sulfate in solution: effects of mono-and divalent salts," Macromolecules **45**, 2882–2890 (2012).

[125] E. Josef and H. Bianco-Peled, "Conformation of a natural polyelectrolyte in semidilute solutions with no added salt," Soft Matter **8**, 9156–9165 (2012).

[126] L. Wang and V. A. Bloomfield, "Small-angle x-ray scattering of semidilute rodlike dna solutions: polyelectrolyte behavior," Macromolecules **24**, 5791–5795 (1991).

[127] R. Borsali, H. Nguyen, and R. Pecora, "Small-angle neutron scattering and dynamic light scattering from a polyelectrolyte solution: Dna," Macromolecules **31**, 1548–1555 (1998).

[128] R. Borsali, M. Rinaudo, and L. Noirez, "Light scattering and small-angle neutron scattering from polyelectrolyte solutions: the succinoglycan," Macromolecules **28**, 1085–1088 (1995).

[129] R. Koyama, "Small-angle scattering of polyelectrolyte solutions," Macromolecules **19**, 178–182 (1986).

[130] K. Nishida, K. Kaji, and T. Kanaya, "Charge density dependence of correlation length due to electrostatic repulsion in polyelectrolyte solutions," Macromolecules **28**, 2472–2475 (1995).

[131] C. G. Lopez, "Entanglement of semiflexible polyelectrolytes: Crossover concentrations and entanglement density of sodium carboxymethyl cellulose," Journal of Rheology **64**, 191–204 (2020).

[132] C. G. Lopez, A. Matsumoto, A. Gulati, C. Hou, Y. Mizutani, H. Osada, Y. Tao, K. Fujii, W. Richtering, and T. Watanabe, "Structure of poly (ionic liquid) s in solutions: a small angle scattering study," (2023).

[133] "This assumes $b = 0.25$ nm for NaPSS. A lower value of 0.17 nm for the effective monomer size was reported by van der Maarel and co-workers which would imply a higher charge density." ().

[134] Note that f is the fraction of monomers with a dissociated charge, not the fraction of dissociated counterions.

[135] E. Dubois and F. Boué, "Conformation of poly (styrenesulfonate) polyions in the presence of multivalent ions: small-angle neutron scattering experiments," Macromolecules **34**, 3684–3697 (2001).

[136] Y. Zhang, J. F. Douglas, B. D. Ermi, and E. J. Amis, "Influence of counterion valency on the scattering properties of highly charged polyelectrolyte solutions," The Journal of Chemical Physics **114**, 3299–3313 (2001).

[137]C. G. Lopez and W. Richtering, "Influence of divalent counterions on the solution rheology and supramolecular aggregation of carboxymethyl cellulose," Cellulose **26**, 1517–1534 (2019).